Hindawi
International Journal of Antennas and Propagation
Volume 2018, Article ID 5247919, 16 pages
https://doi.org/10.1155/2018/5247919

Research Article

Estimation for Two-Dimensional Nonsymmetric Coherently Distributed Source in L-Shaped Arrays

Tao Wu,[1] **Zhenghong Deng**,[1] **Qingyue Gu**,[2] **and Jiwei Xu**[1]

[1]*School of Automation, Northwestern Polytechnical University, Xi'an, Shaanxi 710072, China*
[2]*School of Marine, Northwestern Polytechnical University, Xi'an, Shaanxi 710072, China*

Correspondence should be addressed to Tao Wu; taowu_nwpu@126.com

Received 28 December 2017; Revised 11 April 2018; Accepted 13 June 2018; Published 3 September 2018

Academic Editor: Shiwen Yang

Copyright © 2018 Tao Wu et al. This is an open access article distributed under the Creative Commons Attribution License, which permits unrestricted use, distribution, and reproduction in any medium, provided the original work is properly cited.

We explore the estimation of a two-dimensional (2D) nonsymmetric coherently distributed (CD) source using L-shaped arrays. Compared with a symmetric source, the modeling and estimation of a nonsymmetric source are more practical. A nonsymmetric CD source is established through modeling the deterministic angular signal distribution function as a summation of Gaussian probability density functions. Parameter estimation of the nonsymmetric distributed source is proposed under an expectation maximization (EM) framework. The proposed EM iterative calculation contains three steps in each cycle. Firstly, the nominal azimuth angles and nominal elevation angles of Gaussian components in the nonsymmetric source are obtained from the relationship of rotational invariance matrices. Then, angular spreads can be solved through one-dimensional (1D) searching based on nominal angles. Finally, the powers of Gaussian components are obtained by solving least-squares estimators. Simulations are conducted to verify the effectiveness of the nonsymmetric CD model and estimation technique.

1. Introduction

Although point source models are commonly used in applications such as wireless communications, radar and sonar systems, distributed source models which have considered multipath propagation and the surface features of targets tend to perform better. Position localization estimators based on distributed source models have proved to be more precise in multipath scenarios compared with point source models. With information of surface features, the distributed source models have potential application for high-resolution underwater acoustical imaging.

Sources may be classified into coherently and incoherently distributed sources [1]. A coherently distributed (CD) source is defined as the signal components arriving from different angles within the range of extension that are coherent. For an incoherently distributed (ID) source, these components are uncorrelated. In this paper, the modeling and estimation of a CD source are considered.

Some classical point source estimation techniques have been extended to CD sources. DSPE [1], DISPARE [2], and vec-MUSIC [3] are developed from MUSIC for distributed sources, where parameters are estimated by two-dimensional (2D) spectral searching. In [4], ESPRIT is extended for distributed sources, where the TLS-ESPRIT algorithm is used to estimate nominal angles of sources firstly, and then angular spreads are obtained by one-dimensional (1D) spectral searching. The authors of [5] have developed an efficient DSPE algorithm and proposed generalized beamforming estimators in [6]. Generally, the parameters of CD sources are approximate solutions under the assumption of small angular spreads; some comparative studies on different methods have been proposed. The performance of two beamforming methods is analyzed in [7]. In the presence of model errors, the performance of DSPE algorithm is analyzed in [8], and the performance of MUSIC is analyzed in [9]. Considering mismodeling of the spatial distribution of distributed sources, a robust estimator is proposed in [10] by means of exploiting some properties of the generalized steering vector in the case of CD sources and the covariance matrix in the case of ID sources. All these methods are based on the 1D distributed source models,

which assume that signal sources are in the same plane, where distributed sources are characterized by the nominal direction of arrival (DOA) and angular spread. However, impinging signals are not generally in the same plane but in a three-dimensional space practically. The 2D distributed source models are usually described by the nominal azimuth DOA, nominal elevation DOA, azimuth angular spread, and elevation angular spread. Involving more parameters, 2D CD source estimation problem is more complicated.

Based on DSPE, several spectral searching methods for 2D CD sources have been proposed. In [11–15], algorithms for exponential CD sources are presented under L-shaped arrays, uniform circular arrays, and nested arrays, which transform a four-dimensional parameter searching problem into a 2D parameter searching problem. The authors of [16] have proposed an estimator for Gaussian CD sources under L-shaped arrays.

Using an array with sensors oriented along three axes of the Cartesian coordinates, the authors of [17] have extended the matrix pencil method for 2D Gaussian and Laplacian CD sources. The method needs not spectral searching, but its array structure is not beneficial to engineering realization and its concern is DOAs without angular spreads.

In [18], a sequential one-dimensional searching (SOS) algorithm is proposed for Gaussian CD sources using a pair of uniform circular arrays, which first estimates the nominal elevation by the TLS-ESPRIT method, followed by sequential one-dimensional searching to seek the nominal azimuth. As the method presented in [17], the SOS algorithm only deals with the DOAs.

Several low-complexity algorithms have been presented in [19–24] utilizing two closely spaced parallel ULAs, treble parallel ULAs, and conformal arrays. It is a common characteristic that though preliminary Taylor approximation to generalized steering vectors, the nominal elevation and azimuth are solved under ESPRIT or modified propagator. The authors of [25] have proposed a method using a centrosymmetric crossed array, where DOAs are obtained through the symmetric properties of the special array. These methods need not any spectral searching and it can deal with unknown angular distribution functions. The disadvantage of these algorithms is that angular spreads are not within consideration.

Utilizing two closely spaced parallel ULAs and L-shaped arrays, two estimators for CD noncircular signals are proposed [26, 27] which exhibit better accuracy and resolution compared with circular signals.

Estimation techniques for distributed sources mentioned above are performed based on the assumption that the spatial distributions of sources are symmetric. Nevertheless, scatters are distributed irregularly or nonuniformly around targets; the distributions of scatters in practice are generally nonsymmetric. Considering complexity, people have paid less attention to nonsymmetric distributed sources.

Based on the principle that a nonsymmetric probability distribution can be composed of several symmetric distributions, some methods for 1D nonsymmetric ID sources have been presented. In [28], a nonsymmetric distribution is modeled by two Gaussian distributions. The shape of the nonsymmetric distribution would be figured via the variation of the ratio between two Gaussian distributions. In [29], the Gaussian mixture model (GMM) is employed to characterize the 1D nonsymmetric ID sources, and the expectation maximization (EM) algorithm is applied to solve the problem.

To the best of our knowledge, there are no algorithms for a 2D nonsymmetric distributed source. In this paper, we are concerned on the estimation of a 2D nonsymmetric CD source. Compared with a symmetric source, the modeling and estimation of a nonsymmetric source are more complex. Through modeling the nonsymmetric deterministic angular signal distribution function by Gaussian mixture, we have presented a parameter estimation method under an EM framework based on L-shaped arrays. In general EM frameworks, the maximization step is to maximize the likelihood function to get the best parameters which are hidden in expectation step results. In our method, the DOA parameters of Gaussian components of the 2D CD source are obtained through two approximate rotational invariance relations. By solving least-squares estimators, powers of Gaussian components are obtained.

2. Signal Model

Figure 1 shows the L-shaped array configuration, which uses the *xoy* plane. Each linear array consists of K sensor elements separated by d meters, and the two linear arrays share an origin sensor. Suppose that there is a CD source with a nominal azimuth angle θ and a nominal elevation angle ϕ, $\theta \in [-\pi/2, \pi/2]$ and $\phi \in [0, \pi/2]$. λ is the wavelength of the impinging signal. The CD source is considered as stationary narrowband stochastic process.

The $K \times 1$ output vectors of the arrays X and Y can be expressed as follows:

$$\begin{aligned} \mathbf{x}(t) &= \iint \mathbf{a}(\theta, \phi) s(\theta, \phi, t) d\theta d\phi + \mathbf{n}_x(t), \\ \mathbf{y}(t) &= \iint \mathbf{b}(\theta, \phi) s(\theta, \phi, t) d\theta d\phi + \mathbf{n}_y(t), \end{aligned} \tag{1}$$

where the steering vectors of the arrays X and Y can be expressed as follows:

$$\begin{aligned} \mathbf{a}(\theta, \phi) &= \left[1, e^{j2\pi d \cos\theta \sin\phi/\lambda}, \ldots, e^{j2\pi(K-1)d \cos\theta \sin\phi/\lambda}\right]^{\mathrm{T}}, \\ \mathbf{b}(\theta, \phi) &= \left[1, e^{j2\pi d \sin\theta \sin\phi/\lambda}, \ldots, e^{j2\pi(K-1)d \sin\theta \sin\phi/\lambda}\right]^{\mathrm{T}}. \end{aligned} \tag{2}$$

$s(\theta, \phi, t)$ is the angular signal density function of the distributed source. According to the CD source assumption, $s(\theta, \phi, t)$ can be expressed as

$$s(\theta, \phi, t) = s(t) f(\theta, \phi; \mathbf{u}), \tag{3}$$

where $s(t)$ is a random process, $P = E[|s(t)|^2]$ is the power of the CD source, $f(\theta, \phi; \mathbf{u})$ is the deterministic angular signal distribution function of the CD source, and $\mathbf{u}$ is the parameter set of the function.

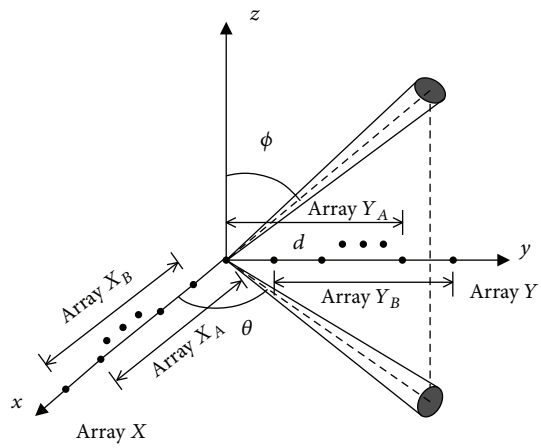

Figure 1: The L-shaped array configuration.

$\mathbf{n}_x(t)$ and $\mathbf{n}_y(t)$ are the $K \times 1$ additive noise vectors which can be combined into

$$\mathbf{n}(t) = \begin{bmatrix} \mathbf{n}_x(t) \\ \mathbf{n}_y(t) \end{bmatrix}. \tag{4}$$

The noise is assumed to be uncorrelated between sensors and Gaussian white with zero mean

$$\begin{aligned} E\left[\mathbf{n}(t)\mathbf{n}^{\mathrm{H}}\left(t'\right)\right] &= \rho \mathbf{I}_{2K}\delta\left(t - t'\right), \\ E\left[\mathbf{n}(t)\mathbf{n}^{\mathrm{T}}\left(t'\right)\right] &= 0 \quad \forall t, t', \end{aligned} \tag{5}$$

where ρ is the noise power, $\mathbf{I}_{2K}$ is the $2K \times 2K$ identity matrix; superscript $(\cdot)^{\mathrm{T}}$ denotes the transpose and $(\cdot)^{\mathrm{H}}$ denotes the Hermitian transpose. $\delta(\cdot)$ is the Kronecker delta function. The signal is assumed to be uncorrelated with the noise.

In this study, the deterministic angular signal distribution function of the CD source can be modeled as a summation of Gaussian distributions in order to express nonsymmetry, so the deterministic angular signal distribution function is obtained as

$$f(\theta, \phi\,; \mathbf{u}) = \sum_{i=1}^{q} w_i g_i(\theta, \phi\,; \mathbf{u}_i), \tag{6}$$

where q is the number of Gaussian components. The ith Gaussian component is defined as

$$g_i(\theta, \phi\,; \mathbf{u}_i) = \frac{1}{2\pi\sigma_{\theta i}\sigma_{\phi i}} \exp\left\{-0.5\left[\left(\frac{\theta - \theta_i}{\sigma_{\theta i}}\right)^2 + \left(\frac{\phi - \phi_i}{\sigma_{\varphi i}}\right)^2\right]\right\}, \tag{7}$$

where $\mathbf{u}_i = [\theta_i, \phi_i, \sigma_{\theta i}, \sigma_{\phi i}]$ is the parameter set with four elements denoting the nominal azimuth, nominal elevation, azimuth angular spread, and elevation angular spread, respectively.

To normalize $f(\theta, \phi\,; \mathbf{u})$, the weighting coefficient w_i satisfies the following constraint:

$$\sum_{i=1}^{q} w_i = 1. \tag{8}$$

The summation of Gaussian distributions in (6) can be substituted for $f(\theta, \phi\,; \mathbf{u})$ in (3) and (1). The output vectors of the arrays X and Y can be expressed as follows:

$$\begin{aligned} \mathbf{x}(t) &= s(t)\sum_{i=1}^{q} w_i \iint \mathbf{a}(\theta, \phi) g_i(\theta, \phi\,; \mathbf{u}_i) d\theta d\phi + \mathbf{n}_x(t), \\ \mathbf{y}(t) &= s(t)\sum_{i=1}^{q} w_i \iint \mathbf{b}(\theta, \phi) g_i(\theta, \phi\,; \mathbf{u}_i) d\theta d\phi + \mathbf{n}_y(t). \end{aligned} \tag{9}$$

3. Proposed Method

The deterministic angular signal distribution function characterized by (6) has $5q$ unknown parameters. Compared with a symmetric CD source, there are much more parameters to be estimated. Due to nonlinear and high-dimensional properties, traditional methods such as maximum likelihood and spectral searching are hard to be used. The EM algorithm [30] is traditionally used to estimate Gaussian mixture parameters. Here, according to the iterative EM optimization framework, an iterative algorithm is presented for estimating the deterministic angular signal distribution function in (6).

3.1. Latent Variable Model. On the basis of the latent variable model described by the authors of [31], the incomplete data is simply the set of observations themselves. The many-to-one function, which is linear and maps the complete data to incomplete data, can be expressed as follows:

$$\begin{aligned} \mathbf{x}(t) &= \sum_{i=1}^{q} \mathbf{x}_i(t), \\ \mathbf{y}(t) &= \sum_{i=1}^{q} \mathbf{y}_i(t). \end{aligned} \tag{10}$$

Define the generalized steering vectors of the complete data for arrays X and Y as follows:

$$\begin{aligned} \boldsymbol{\alpha}_i(\mathbf{u}_i) &= \iint \mathbf{a}(\theta, \phi) g_i(\theta, \phi\,; \mathbf{u}_i) d\theta d\phi, \\ \boldsymbol{\beta}_i(\mathbf{u}_i) &= \iint \mathbf{b}(\theta, \phi) g_i(\theta, \phi\,; \mathbf{u}_i) d\theta d\phi. \end{aligned} \tag{11}$$

Combine the incomplete data $\mathbf{x}(t)$ and $\mathbf{y}(t)$ into

$$\mathbf{z}(t) = \begin{bmatrix} \mathbf{x}(t) \\ \mathbf{y}(t) \end{bmatrix} = s(t) \begin{bmatrix} \sum_{i=1}^{q} w_i \boldsymbol{\alpha}_i(\mathbf{u}_i) \\ \sum_{i=1}^{q} w_i \boldsymbol{\beta}_i(\mathbf{u}_i) \end{bmatrix} + \begin{bmatrix} \mathbf{n}_x(t) \\ \mathbf{n}_y(t) \end{bmatrix}. \tag{12}$$

The noise is assumed to be distributed in the complete data equally. Combine the complete data $\mathbf{x}_i(t)$ and $\mathbf{y}_i(t)$ into

$$\mathbf{z}_i(t) = \begin{bmatrix} \mathbf{x}_i(t) \\ \mathbf{y}_i(t) \end{bmatrix} = s(t) \begin{bmatrix} w_i \boldsymbol{\alpha}_i(\mathbf{u}_i) \\ w_i \boldsymbol{\beta}_i(\mathbf{u}_i) \end{bmatrix} + \frac{1}{q} \begin{bmatrix} \mathbf{n}_x(t) \\ \mathbf{n}_y(t) \end{bmatrix}. \tag{13}$$

Define two data selection matrices as follows:

$$\begin{aligned} \mathbf{A} &= \left[\mathbf{I}_{(K-1)\times(K-1)} \mid \mathbf{0}_{(K-1)\times 1} \right], \\ \mathbf{B} &= \left[\mathbf{0}_{(K-1)\times 1} \mid \mathbf{I}_{(K-1)\times(K-1)} \right], \end{aligned} \tag{14}$$

where $\mathbf{I}_{(K-1)\times(K-1)}$ is the $(K-1)\times(K-1)$ identity matrix and $\mathbf{0}_{(K-1)\times 1}$ is the $(K-1)\times 1$ zero matrix. Divide X into two shifted subarrays X_A and X_B, and divide Y into two shifted subarrays Y_A and Y_B, which are depicted in Figure 1.

The output vectors of the subarrays X_A, X_B, Y_A, and Y_B can be expressed as

$$[\mathbf{x}_A(t), \mathbf{x}_B(t), \mathbf{y}_A(t), \mathbf{y}_B(t)] = [\mathbf{A}\mathbf{x}(t), \mathbf{B}\mathbf{x}(t), \mathbf{A}\mathbf{y}(t), \mathbf{B}\mathbf{y}(t)]. \tag{15}$$

The complete data of output vectors of the subarrays X_A, X_B, Y_A, and Y_B is obtained as

$$[\mathbf{x}_{Ai}(t), \mathbf{x}_{Bi}(t), \mathbf{y}_{Ai}(t), \mathbf{y}_{Bi}(t)] = [\mathbf{A}\mathbf{x}_i(t), \mathbf{B}\mathbf{x}_i(t), \mathbf{A}\mathbf{y}_i(t), \mathbf{B}\mathbf{y}_i(t)]. \tag{16}$$

The generalized steering vectors of the complete data for X_A, X_B, Y_A, and Y_B can be written as

$$[\boldsymbol{\alpha}_{Ai}(\mathbf{u}_i), \boldsymbol{\alpha}_{Bi}(\mathbf{u}_i), \boldsymbol{\beta}_{Ai}(\mathbf{u}_i), \boldsymbol{\beta}_{Bi}(\mathbf{u}_i)] = [\mathbf{A}\boldsymbol{\alpha}_i(\mathbf{u}_i), \mathbf{B}\boldsymbol{\alpha}_i(\mathbf{u}_i), \mathbf{A}\boldsymbol{\beta}_i(\mathbf{u}_i), \mathbf{B}\boldsymbol{\beta}_i(\mathbf{u}_i)]. \tag{17}$$

Assume that the angular spreads of Gaussian angular signal distribution in the complete data are small. The authors of [19] have proved that for $d/\lambda = 1/2$, there exists an approximate rotational invariance relation as follows (see Appendix A):

$$\begin{aligned} \boldsymbol{\alpha}_{Ai}(\mathbf{u}_i) &\approx e^{j\pi \cos\theta_i \sin\phi_i} \boldsymbol{\alpha}_{Bi}(\mathbf{u}_i), \\ \boldsymbol{\beta}_{Ai}(\mathbf{u}_i) &\approx e^{j\pi \sin\theta_i \sin\phi_i} \boldsymbol{\beta}_{Bi}(\mathbf{u}_i). \end{aligned} \tag{18}$$

3.2. EM Algorithm. The sample covariance matrices of the complete data $\bar{\mathbf{R}}_{xi}$ and $\bar{\mathbf{R}}_{yi}$ with N snapshots are defined as follows:

$$\begin{aligned} \bar{\mathbf{R}}_{xi} &= \sum_{t=1}^{N} \mathbf{x}_i(t)\mathbf{x}_i(t)^{\mathrm{H}}, \\ \bar{\mathbf{R}}_{yi} &= \sum_{t=1}^{N} \mathbf{y}_i(t)\mathbf{y}_i(t)^{\mathrm{H}}, \end{aligned} \tag{19}$$

while the sample covariance matrix $\bar{\mathbf{R}}_{zi}$ with N snapshots is defined as

$$\bar{\mathbf{R}}_{zi} = \sum_{t=1}^{N} \begin{bmatrix} \mathbf{x}_i(t) \\ \mathbf{y}_i(t) \end{bmatrix} \begin{bmatrix} \mathbf{x}_i(t) \\ \mathbf{y}_i(t) \end{bmatrix}^{\mathrm{H}}. \tag{20}$$

The negative logarithm of the likelihood function can be simplified as

$$L(w_i, \mathbf{u}_i) = \log |\mathbf{R}_{zi}| + \mathrm{tr}\left(\mathbf{R}_{zi}^{-1} \bar{\mathbf{R}}_{zi}\right), \tag{21}$$

where the covariance matrix of the complete data $\mathbf{z}_i(t)$ can be expressed as

$$\mathbf{R}_{zi} = E\left[\mathbf{z}_i(t)\mathbf{z}_i(t)^{\mathrm{H}}\right] = P_i \begin{bmatrix} \boldsymbol{\alpha}_i(\mathbf{u}_i) \\ \boldsymbol{\beta}_i(\mathbf{u}_i) \end{bmatrix} \begin{bmatrix} \boldsymbol{\alpha}_i(\mathbf{u}_i) \\ \boldsymbol{\beta}_i(\mathbf{u}_i) \end{bmatrix}^{\mathrm{H}} + \rho_i. \tag{22}$$

In formula (22), P_i is the power of the ith complete data. $\rho_i = \rho/q^2$ is the noise power in the ith complete data. From formulas (12) and (13), $\mathbf{z}_i(t)$ can be denoted as

$$\mathbf{z}_i(t) = \begin{bmatrix} \mathbf{x}_i(t) \\ \mathbf{y}_i(t) \end{bmatrix} = s(t) \begin{bmatrix} w_i \boldsymbol{\alpha}_i(\mathbf{u}_i) \\ w_i \boldsymbol{\beta}_i(\mathbf{u}_i) \end{bmatrix} + \frac{1}{q} \begin{bmatrix} \mathbf{x}(t) - \sum_{i=1}^{q} s(t) w_i \boldsymbol{\alpha}_i(\mathbf{u}_i) \\ \mathbf{y}(t) - \sum_{i=1}^{q} s(t) w_i \boldsymbol{\beta}_i(\mathbf{u}_i) \end{bmatrix}. \tag{23}$$

As $\bar{\mathbf{R}}_{zi}$ is a sufficient statistic of w_i, θ_i, ϕ_i, σ_i, and P_i, the m th expectation step of the EM algorithm serves to calculate the expected value of the sufficient statistic as

$$\bar{\mathbf{R}}_{zi}^{m} = (w_i^m)^2 P^m \begin{bmatrix} \boldsymbol{\alpha}_i(\mathbf{u}_i^m) \\ \boldsymbol{\beta}_i(\mathbf{u}_i^m) \end{bmatrix} \begin{bmatrix} \boldsymbol{\alpha}_i(\mathbf{u}_i^m) \\ \boldsymbol{\beta}_i(\mathbf{u}_i^m) \end{bmatrix}^{\mathrm{H}} + \frac{1}{q^2} \begin{bmatrix} \bar{\mathbf{R}}_x - P^m \sum_{i=1}^{q} w_i^m \boldsymbol{\alpha}_i(\mathbf{u}_i^m) \sum_{i=1}^{q} w_i^m \boldsymbol{\alpha}_i^{\mathrm{H}}(\mathbf{u}_i^m) & \bar{\mathbf{R}}_{xy} - P^m \sum_{i=1}^{q} w_i^m \boldsymbol{\alpha}_i(\mathbf{u}_i^m) \sum_{i=1}^{q} w_i^m \boldsymbol{\beta}_i^{\mathrm{H}}(\mathbf{u}_i^m) \\ \bar{\mathbf{R}}^{\mathrm{H}}{}_{xy} - P^m \sum_{i=1}^{q} w_i^m \boldsymbol{\beta}_i(\mathbf{u}_i^m) \sum_{i=1}^{q} w_i^m \boldsymbol{\alpha}_i^{\mathrm{H}}(\mathbf{u}_i^m) & \bar{\mathbf{R}}_y - P^m \sum_{i=1}^{q} w_i^m \boldsymbol{\beta}_i(\mathbf{u}_i^m) \sum_{i=1}^{q} w_i^m \boldsymbol{\beta}_i^{\mathrm{H}}(\mathbf{u}_i^m) \end{bmatrix}, \tag{24}$$

where the superscript m denotes the value of variables at the mth iteration. The sample covariance matrices $\bar{\mathbf{R}}_x$, $\bar{\mathbf{R}}_y$, and $\bar{\mathbf{R}}_{xy}$ with N snapshots are defined as

$$\begin{aligned}\bar{\mathbf{R}}_x &= \frac{1}{N}\sum_{t=1}^{N}\mathbf{x}(t)\mathbf{x}(t)^{\mathrm{H}},\\ \bar{\mathbf{R}}_y &= \frac{1}{N}\sum_{t=1}^{N}\mathbf{y}(t)\mathbf{y}(t)^{\mathrm{H}},\\ \bar{\mathbf{R}}_{xy} &= \frac{1}{N}\sum_{t=1}^{N}\mathbf{x}(t)\mathbf{y}(t)^{\mathrm{H}}.\end{aligned} \tag{25}$$

To simplify the estimation, we assume that the azimuth angular spread and elevation angular spread are the same; σ_i is used to replace $\sigma_{\theta i}$ and $\sigma_{\phi i}$ for convenience. The maximization step will minimize the objective function (21) to find the optimal parameters in the $(m+1)$th iteration. The function (21) can be expressed as

$$w_i^{m+1}, \theta_i^{m+1}, \phi_i^{m+1}, \sigma_i^{m+1}, P_i^{m+1} = \underset{w_i,\mathbf{u}_i}{\operatorname{argmin}}\left[\log|\mathbf{R}_{zi}| + \operatorname{tr}\left(\mathbf{R}_{zi}^{-1}\bar{\mathbf{R}}_{zi}^{m}\right)\right], \tag{26}$$

which means exploring the best $(m+1)$th parameters of the ith Gaussian component based on the sample covariance matrix of the complete data $\bar{\mathbf{R}}_{zi}^{m}$ obtained in the mth iteration. Minimizing (26) is too computationally complex mainly because it is nonlinear and involves a high dimensional matrix inversion. According to the rotational invariance relation, we can firstly estimate the nominal azimuth and nominal elevation of the complete data and then solve other parameters successively based on parameters that have been solved.

The sample covariance matrix of the complete data $\mathbf{x}_i(t)$ and $\mathbf{y}_i(t)$ can be obtained as follows:

$$\begin{aligned}\bar{\mathbf{R}}_{xi}^{m} &= \begin{bmatrix}\mathbf{I}_{K\times K} & \mathbf{0}_{K\times K}\\ \mathbf{0}_{K\times K} & \mathbf{0}_{K\times K}\end{bmatrix}\bar{\mathbf{R}}_{zi}^{m},\\ \bar{\mathbf{R}}_{yi}^{m} &= \begin{bmatrix}\mathbf{0}_{K\times K} & \mathbf{0}_{K\times K}\\ \mathbf{0}_{K\times K} & \mathbf{I}_{K\times K}\end{bmatrix}\bar{\mathbf{R}}_{zi}^{m},\end{aligned} \tag{27}$$

where $\mathbf{I}_{K\times K}$ is the $K\times K$ identity matrix and $\mathbf{0}_{K\times K}$ is the $K\times K$ zero matrix. By means of eigendecomposition of the covariance matrices $\bar{\mathbf{R}}_{xi}^{m}$ and $\bar{\mathbf{R}}_{yi}^{m}$, we obtain

$$\begin{aligned}\bar{\mathbf{R}}_{xi}^{m} &= c\mathbf{E}_{xi}^{m}(\mathbf{E}_{xi}^{m})^{\mathrm{H}} + \rho_i\mathbf{N}_{xi}^{m}(\mathbf{N}_{xi}^{m})^{\mathrm{H}},\\ \bar{\mathbf{R}}_{yi}^{m} &= c\mathbf{E}_{yi}^{m}\left(\mathbf{E}_{yi}^{m}\right)^{\mathrm{H}} + \rho_i\mathbf{N}_{yi}^{m}\left(\mathbf{N}_{yi}^{m}\right)^{\mathrm{H}},\end{aligned} \tag{28}$$

where c is a constant, $\mathbf{E}_{xi}^{m}$ and $\mathbf{E}_{yi}^{m}$ are the K-dimensional eigenvectors of $\bar{\mathbf{R}}_{xi}^{m}$ and $\bar{\mathbf{R}}_{yi}^{m}$ corresponding to the largest eigenvalues, respectively, while $\mathbf{N}_{xi}^{m}$ and $\mathbf{N}_{yi}^{m}$ are the $K\times(K-1)$ matrices representing noise subspace.

Let $\mathbf{E}_{xAi}^{m}$ and $\mathbf{E}_{xBi}^{m}$ be the upper $(K-1)$ and the lower $(K-1)$ elements of $\mathbf{E}_{xi}^{m}$, respectively, corresponding to the subarrays X_A and X_B; $\mathbf{E}_{yAi}^{m}$ and $\mathbf{E}_{yBi}^{m}$ are the upper $(K-1)$ and the lower $(K-1)$ elements of $\mathbf{E}_{yi}^{m}$, respectively, corresponding to the subarrays Y_A and Y_B. There exist relationships as follows:

$$\begin{aligned}\mathbf{E}_{xi}^{m} &= \begin{bmatrix}\text{the first row}\\ \mathbf{E}_{xBi}^{m}\end{bmatrix} = \begin{bmatrix}\mathbf{E}_{xAi}^{m}\\ \text{the last row}\end{bmatrix}\\ &= \begin{bmatrix}\text{the first row}\\ \boldsymbol{\alpha}_{Bi}(\mathbf{u}_i)\end{bmatrix}c' = \begin{bmatrix}\boldsymbol{\alpha}_{Ai}(\mathbf{u}_i)\\ \text{the last row}\end{bmatrix}c',\\ \mathbf{E}_{yi}^{m} &= \begin{bmatrix}\text{the first row}\\ \mathbf{E}_{yBi}^{m}\end{bmatrix} = \begin{bmatrix}\mathbf{E}_{yAi}^{m}\\ \text{the last row}\end{bmatrix}\\ &= \begin{bmatrix}\text{the first row}\\ \boldsymbol{\beta}_{Bi}(\mathbf{u}_i)\end{bmatrix}c'' = \begin{bmatrix}\boldsymbol{\beta}_{Ai}(\mathbf{u}_i)\\ \text{the last row}\end{bmatrix}c'',\end{aligned} \tag{29}$$

where c' and c'' are constants. Let $h_i = \cos\theta_i \sin\phi_i$ and $v_i = \sin\theta_i \sin\phi_i$.

From formula (29), we have

$$\begin{aligned}h_i^{m+1} &= \ln\frac{\mathbf{1}_{1\times(K-1)}\times(\mathbf{E}_{xBi}^{m}./\mathbf{E}_{xAi}^{m})}{j\pi(K-1)},\\ v_i^{m+1} &= \ln\frac{\mathbf{1}_{1\times(K-1)}\times\left(\mathbf{E}_{yB_i}^{m}./\mathbf{E}_{yA_i}^{m}\right)}{j\pi(K-1)},\end{aligned} \tag{30}$$

where $\mathbf{I}_{1\times(K-1)}$ is the $1\times(K-1)$ identity matrix and $(./)$ denotes the element-wise division operation. The nominal azimuth and nominal elevation of the complete data in the $(m+1)$th maximization step can be obtained from

$$\begin{aligned}\phi_i^{m+1} &= \arcsin\left(\sqrt{\left(h_i^{m+1}\right)^2 + \left(v_i^{m+1}\right)^2}\right),\\ \theta_i^{m+1} &= \arctan\left(\frac{v_i^{m+1}}{h_i^{m+1}}\right).\end{aligned} \tag{31}$$

According to the orthogonality of the subspace, σ_i can be obtained from one-dimensional searching

$$\begin{aligned}\sigma_i^{m+1} = \arg\min\ &\left[\boldsymbol{\alpha}_i\left(\theta_i^{m+1},\phi_i^{m+1},\sigma_i\right)^{\mathrm{H}}, \boldsymbol{\beta}_i\left(\theta_i^{m+1},\phi_i^{m+1},\sigma_i\right)^{\mathrm{H}}\right]\\ &\cdot\begin{bmatrix}\mathbf{N}_{xi}^{m}\\ \mathbf{N}_{yi}^{m}\end{bmatrix}\begin{bmatrix}\mathbf{N}_{xi}^{m}\\ \mathbf{N}_{yi}^{m}\end{bmatrix}^{\mathrm{H}}\\ &\cdot\left[\boldsymbol{\alpha}_i\left(\theta_i^{m+1},\phi_i^{m+1},\sigma_i\right)^{\mathrm{H}}, \boldsymbol{\beta}_i\left(\theta_i^{m+1},\phi_i^{m+1},\sigma_i\right)^{\mathrm{H}}\right]^{\mathrm{H}}.\end{aligned} \tag{32}$$

Under the condition that the parameters nominal azimuth θ_i, nominal elevation ϕ_i, angular spread σ_i are solved, the generalized steering vectors of complete data can be expressed as follows (see Appendix B):

$$\begin{aligned}\left[\boldsymbol{\alpha}_i(\mathbf{u}_i)\right]_k &= e^{j\pi(k-1)\cos\theta_i \sin\phi_i} e^{-0.5\left\{[\pi\sigma_i(k-1)\sin\theta_i\sin\phi_i]^2+[\pi\sigma_i(k-1)\cos\theta_i\cos\phi_i]^2\right\}},\\ \left[\boldsymbol{\beta}_i(\mathbf{u}_i)\right]_k &= e^{j\pi(k-1)\sin\theta_i \sin\phi_i} e^{-0.5\left\{[\pi\sigma_i(k-1)\cos\theta_i\sin\phi_i]^2+[\pi\sigma_i(k-1)\sin\theta_i\cos\phi_i]^2\right\}}.\end{aligned} \tag{33}$$

The least-squares fits of the theoretical and sample covariance can be expressed as

$$U = \left\|\bar{R}_{zi} - P_i\mathbf{r}_i(\mathbf{u}_i) - \rho_i\mathbf{I}_{2K}\right\|_{\mathrm{F}}^2, \tag{34}$$

where

$$\mathbf{r}_i(\mathbf{u}_i) = \begin{bmatrix}\boldsymbol{\alpha}_i(\mathbf{u}_i)\\ \boldsymbol{\beta}_i(\mathbf{u}_i)\end{bmatrix}\begin{bmatrix}\boldsymbol{\alpha}_i(\mathbf{u}_i)\\ \boldsymbol{\beta}_i(\mathbf{u}_i)\end{bmatrix}^{\mathrm{H}}. \tag{35}$$

Differentiating (34) with respect to P_i and ϱ_i setting the results to zero yield the following equation:

$$\rho_i = \frac{\mathrm{tr}\left(\bar{\mathbf{R}}_{zi}\right)\mathrm{tr}\left[\mathbf{r}_i(\mathbf{u}_i)\mathbf{r}_i(\mathbf{u}_i)^*\right] - \mathrm{tr}\left[\mathbf{r}_i(\mathbf{u}_i)\bar{\mathbf{R}}_{zi}^*\right]\mathrm{tr}\left[\mathbf{r}_i(\mathbf{u}_i)\right]}{2K\mathrm{tr}\left[\mathbf{r}_i(\mathbf{u}_i)\mathbf{r}_i(\mathbf{u}_i)^*\right] - \mathrm{tr}\left[\mathbf{r}_i(\mathbf{u}_i)\right]\mathrm{tr}\left[\mathbf{r}_i(\mathbf{u}_i)\right]}, \tag{36}$$

$$P_i = \frac{2K\mathrm{tr}\left[\mathbf{r}_i(\mathbf{u}_i)\bar{\mathbf{R}}_{zi}^*\right] - \mathrm{tr}\left[\mathbf{r}_i(\mathbf{u}_i)\right]\mathrm{tr}\left(\bar{\mathbf{R}}_{zi}\right)}{2K\mathrm{tr}\left[\mathbf{r}_i(\mathbf{u}_i)\mathbf{r}_i(\mathbf{u}_i)^*\right] - \mathrm{tr}\left[\mathbf{r}_i(\mathbf{u}_i)\right]\mathrm{tr}\left[\mathbf{r}_i(\mathbf{u}_i)\right]}, \tag{37}$$

where superscript $(\cdot)^*$ denotes the conjugate operation and $\mathrm{tr}(\cdot)$ is the trace of matrix.

Let

$$\gamma_\tau^{m+1} = \sqrt{\frac{P_i^{m+1}}{P_{i+1}^m}}, \quad \tau = i \ \text{ when } i < q. \tag{38}$$

From $P_i = P/w_i^2$ and formula (8), we can get

$$w_i^{m+1} = \begin{cases}\dfrac{\prod_{\tau=i}^{q-1}\gamma_\tau^{m+1}}{\prod_{\tau=1}^{q-1}\gamma_\tau^{m+1} + \prod_{\tau=2}^{q-1}\gamma_\tau^{m+1} + \cdots + \gamma_{q-1}^{m+1} + 1} & (1 \le i < q),\\ \dfrac{1}{\prod_{\tau=1}^{q-1}\gamma_i^{m+1} + \prod_{\tau=2}^{q-1}\gamma_i^{m+1} + \cdots + \gamma_{q-1}^{m+1} + 1} & (i = q).\end{cases} \tag{39}$$

At last, the power of the CD source can be obtained from

$$P^{m+1} = \frac{P_i^{m+1}}{\left(w_i^{m+1}\right)^2}. \tag{40}$$

3.3. Complexity Analysis and Comparison. Now, we analyze the computational complexity of the proposed method in comparison with DSPE [16] and TLS-ESPRIT [19] which are two estimators for 2D symmetric CD sources under L-shaped arrays. The DSPE method estimates DOAs and angular spreads through two 2D spectral searches; its computation cost is mostly made of three parts: the calculation of the sample covariance matrix, the eigendecomposition of the matrix, and 2D searching. TLS-ESPRIT [19] is a method of DOA estimation; its computational cost mostly consists of the estimation and eigendecomposition of a $2K \times 2K$ sample covariance matrix.

The stopping criterion of the EM algorithm is all parameters no longer changing [30, 31]. We define the iterative variation of all parameters as

$$\delta = \frac{1}{4q}\left|\frac{\varepsilon_\mu^{m+1} - \varepsilon_\mu^m}{\varepsilon_\mu^m}\right|, \quad \mu = 1, 2, \ldots, 4q, \tag{41}$$

where ε_μ^m represents a parameter value in the mth iteration. When δ reaches a sufficiently small value, all parameters can be considered keeping stable. The computation cost of the proposed method in one EM circle mainly consists of three parts: the calculation of the $2K \times 2K$ sample covariance matrix, the eigendecomposition of the matrix, and 1D searching. Assume that M is the EM iteration number. Table 1 shows the main computational cost of three methods. From Table 1, we can clearly obtain that the computational cost of the estimation for a nonsymmetric distributed source is significantly higher than that of a symmetric distributed source.

Now, our algorithm can be summarized as follows.

Step1. Determine the number of components q, and initialize P, w_i, θ_i, ϕ_i, and $\sigma_i (i = 1, 2, \ldots, q)$.

Step2. Repeat the following substeps for M times which is a given sufficiently large number or until the iterative variation of all parameters reaches the condition $\delta \le 0.01$.

(1) Compute the sample covariance matrices of complete data $\bar{\mathbf{R}}_{zi}^m$, $\bar{\mathbf{R}}_{xi}^m$, and $\bar{\mathbf{R}}_{yi}^m$ using (24) and (27).

(2) Find the eigenvectors $\mathbf{E}_{xi}^m$ and $\mathbf{E}_{yi}^m$ corresponding to the largest eigenvalues through the eigendecomposition of $\bar{\mathbf{R}}_{xi}^m$ and $\bar{\mathbf{R}}_{yi}^m$.

(3) Calculate the nominal azimuth θ_i^{m+1}, nominal elevation ϕ_i^{m+1}, and angular spread σ_i^{m+1} from (30), (31), and (32).

Table 1: Computational complexity of different methods.

Method	Calculation of the sample covariance matrix	Eigendecomposition	Searching	Total
DSPE	$o(4NK^2)$	$o(8K^3)$	$o(24K^3)$	$o(4NK^2) + o(8K^3) + o(24K^3)$
TLS-ESPRIT	$o(4NK^2)$	$o(8K^3)$		$o(4NK^2) + o(8K^3)$
Proposed	$o(4MNK^2)$	$o(8MK^3)$	$o[M(8K^2 + 2K - 1)(2K - 1)]$	o $(4MNK^2) + o(8MK^3) + o[M(8K^2 + 2K - 1)(2K - 1)]$

(4) Estimate the power of each component P_i^{m+1} using (37), calculate the weight of each component w_i^{m+1} using (39), and get the power of the distributed source from (40).

(5) Repeat substeps 1 to 4 for $i = 1, 2, \ldots, q$.

It is noteworthy that the initial positions of the Gaussian components can be obtained by existing algorithms for a symmetric CD source and set uniformly around the guessed values. The distribution of a 2D nonsymmetric CD source is unknown so the true number of Gaussian components q is unknown; q needs to be set at a reasonable value initially. In the next section, the influence of initial parameters on estimation performance will be discussed.

4. Numerical Results

In this section, four simulation experiments are conducted to verify the effectiveness of the proposed technique. We consider the array geometry as depicted in Figure 1 with $K = 4$ sensors in both the x-axis and y-axis. d/λ is set at 1/2. SNR is defined as

$$\text{SNR} = 10 \log \frac{P}{\rho}. \tag{42}$$

We use the root-mean-squared error (RMSE) to evaluate the estimation performance. The RMSE of the nominal angles is defined as

$$\text{RMSE}_a = \sqrt{\frac{1}{\text{Mc}} \sum_{\varsigma}^{\text{Mc}} \left(\widehat{\theta}^{\varsigma} - \theta\right)^2 + \frac{1}{\text{Mc}} \sum_{\varsigma}^{\text{Mc}} \left(\widehat{\varphi}^{\varsigma} - \phi\right)^2}, \tag{43}$$

where $\widehat{\theta}^{\varsigma}$ and $\widehat{\phi}^{\varsigma}$ are the estimated nominal azimuth and estimated nominal elevation of the CD source, respectively. The superscript ς denotes the estimated parameters from the ςth Monte Carlo run. Mc is the number of Monte Carlo simulations which is set at 500. Additionally, θ and ϕ are the true nominal azimuth and nominal elevation, respectively.

The nominal angle in the proposed algorithm is defined as the value corresponding to the maximum point of the deterministic angular signal distribution function, which can be obtained by the partial derivative of the function.

To examine the difference between the estimated and true nonsymmetric distributed source, the estimation of nominal angles is only part of the problem; in addition, the spatial distribution of the source should be emphasized compared with the estimation of a symmetric distributed source. To evaluate the estimation of the spatial distribution, the RMSE of the distributed function is defined as

$$\text{RMSE}_f = \sqrt{\frac{1}{\text{Mc}} \sum_{\varsigma}^{\text{Mc}} \iint \left[f(\theta, \phi; \widehat{\mathbf{u}}^{\varsigma}) - f(\theta, \phi; \mathbf{u})\right]^2 d\theta d\phi}, \tag{44}$$

where $f(\theta, \phi; \widehat{\mathbf{u}}^{\varsigma})$ is the estimated deterministic angular signal distribution function from the ςth Monte Carlo run. In this section, we compare the performance of the proposed algorithm with DSPE [16] and TLS-ESPRIT [19] for a constructed 2D nonsymmetric CD source with the deterministic angular signal distribution function as

$$\begin{aligned} f(\theta, \phi; \mathbf{u}) = {} & 0.2g(40, 40, 2.5) + 0.2g(45, 40, 2.5) \\ & + 0.2g(50, 40, 2.5) + 0.3g(40, 45, 2.5) \\ & + 0.1g(40, 50, 3), \end{aligned} \tag{45}$$

where $g(a_1, a_2, a_3)$ denotes a Gaussian component

$$g(a_1, a_2, a_3) = \frac{1}{2\pi a_3^2} \exp\left\{0.5\left[\left(\frac{\theta - a_1}{a_3}\right)^2 + \left(\frac{\phi - a_2}{a_3}\right)^2\right]\right\}. \tag{46}$$

Figure 2 shows the constructed nonsymmetric angular signal distribution function which needs to be estimated.

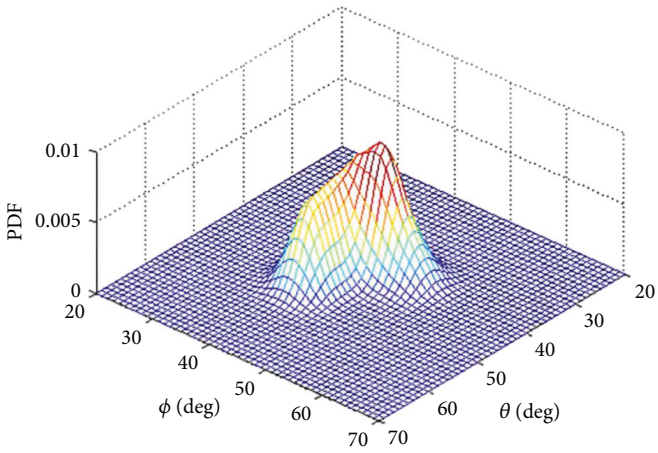

Figure 2: Probability density function (PDF) of the constructed nonsymmetric angular signal distribution.

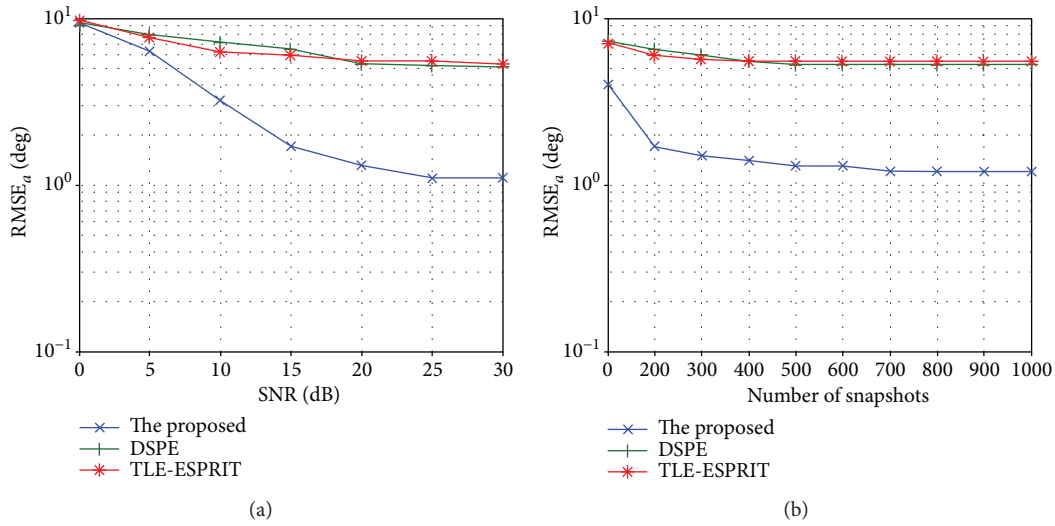

Figure 3: (a) RMSE$_a$ estimated by the three methods versus SNR; (b) RMSE$_a$ estimated by the three methods versus number of snapshots.

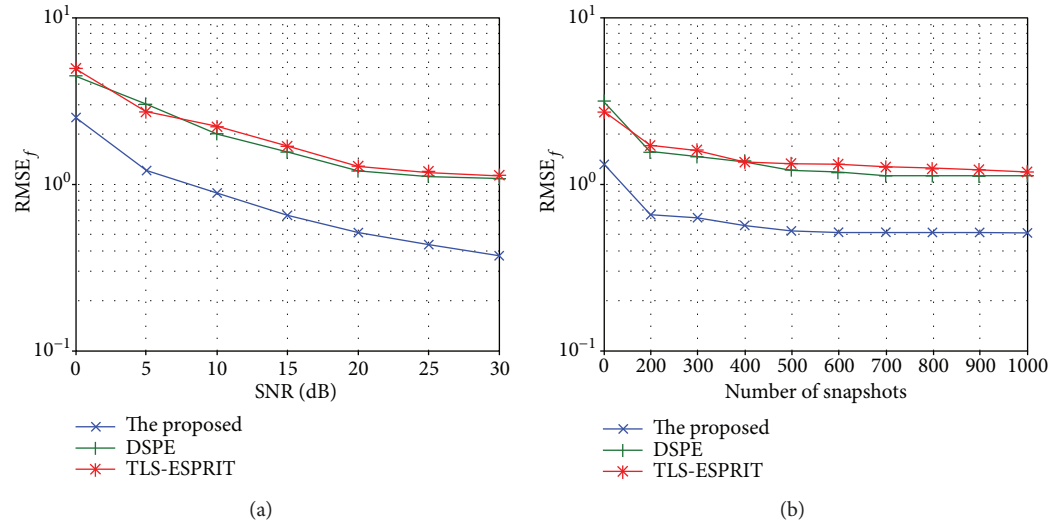

Figure 4: (a) RMSE$_f$ estimated by the three methods versus SNR; (b) RMSE$_f$ estimated by the three methods versus number of snapshots.

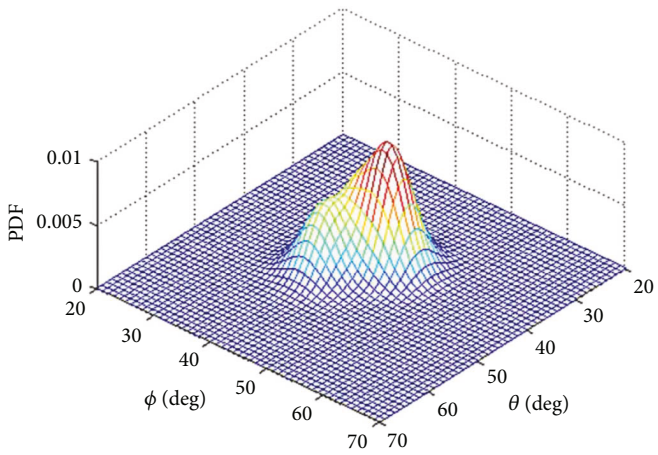

Figure 5: The estimation of nonsymmetric angular signal distribution function by the proposed method.

In the first example, we investigate the performance of the proposed method as well as a comparison with DSPE and TLS-ESPRIT. Figures 3(a) and 3(b) display the estimation of RMSE$_a$ by the proposed algorithm, DSPE, as well as TLS-ESPRIT, while Figures 4(a) and 4(b) show the estimation of RMSE$_f$. Figure 3(a) and 4(a) investigate the influence of SNR on performance with the number of snapshots N = 200 while Figure 3(b) and 4(b) show the influence of the number of snapshots with SNR = 15 dB. The EM iteration number M is set at 200. It can be observed that all algorithms perform better as the number of snapshots or SNR increases. Clearly, the proposed algorithm provides better performance than other estimators with regard to RMSE$_a$ and especially to RMSE$_f$. From Figures 4(a) and 4(b), we can find that there exists a big error of RMSE$_f$ by DSPE and TLS-ESPRIT. It can be concluded that utilizing traditional symmetric estimators for a nonsymmetric distributed source is invalid. Figure 5 displays the estimation of the deterministic angular

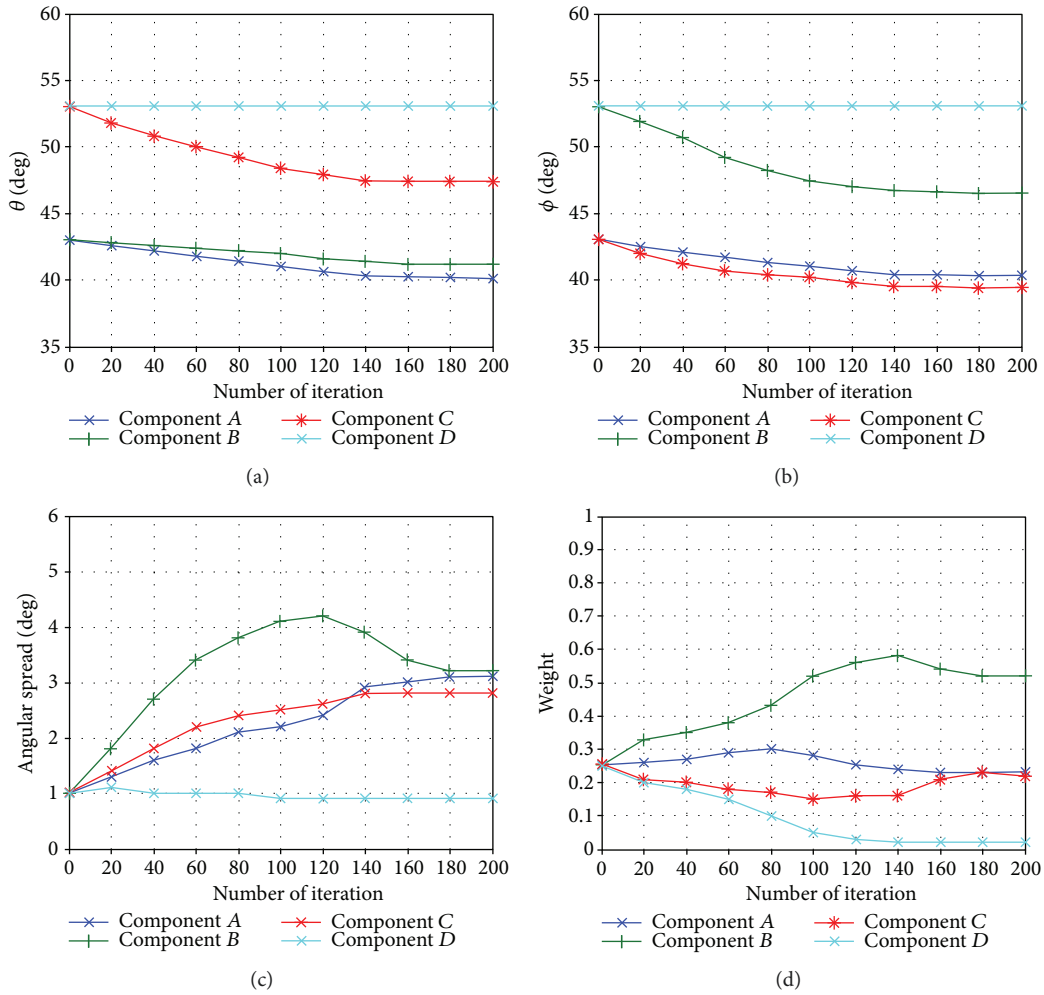

Figure 6: (a) The changing process of central azimuths in EM iterations; (b) the changing process of central elevations in EM iterations; (c) the changing process of angular spreads in EM iterations; (d) the changing process of weights in EM iterations.

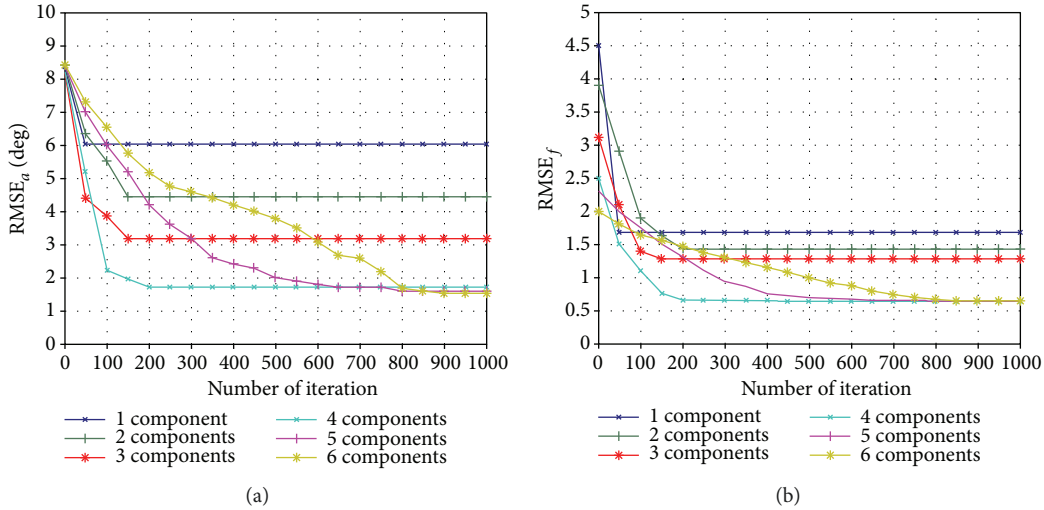

Figure 7: (a) RMSE$_a$ estimated by different numbers of Gaussian components; (b) RMSE$_f$ estimated by different numbers of Gaussian components.

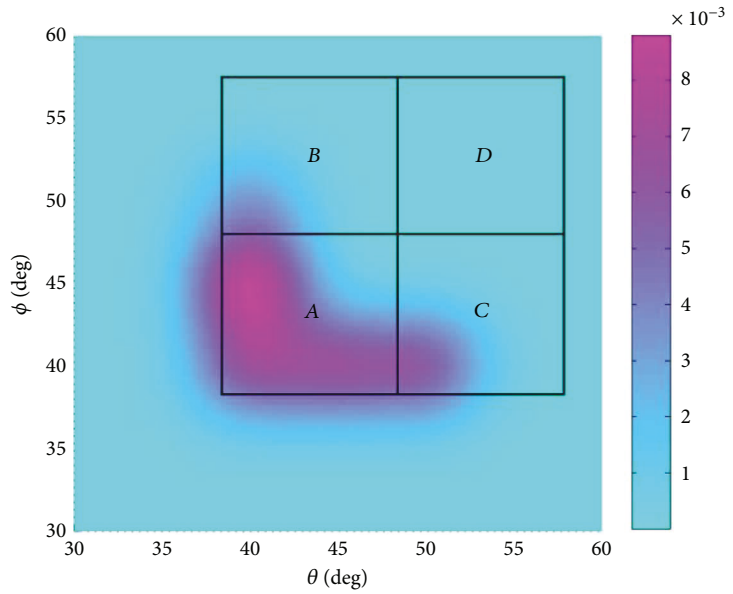

Figure 8: Squares of taking initial positions for each component.

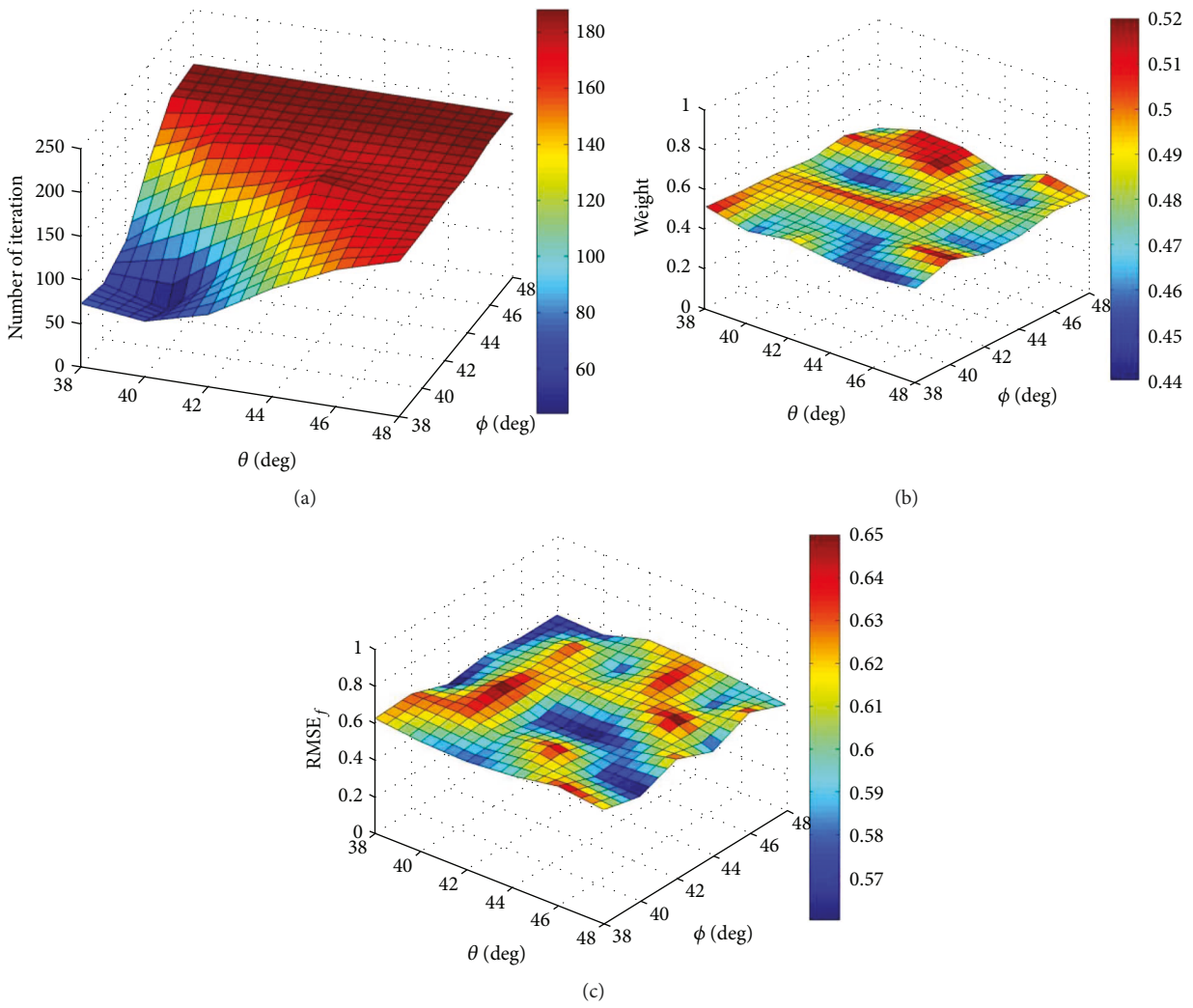

Figure 9: (a) Number of iteration versus initial position for component A; (b) weight versus initial position for component A; (c) RMSE$_f$ versus initial position for component A.

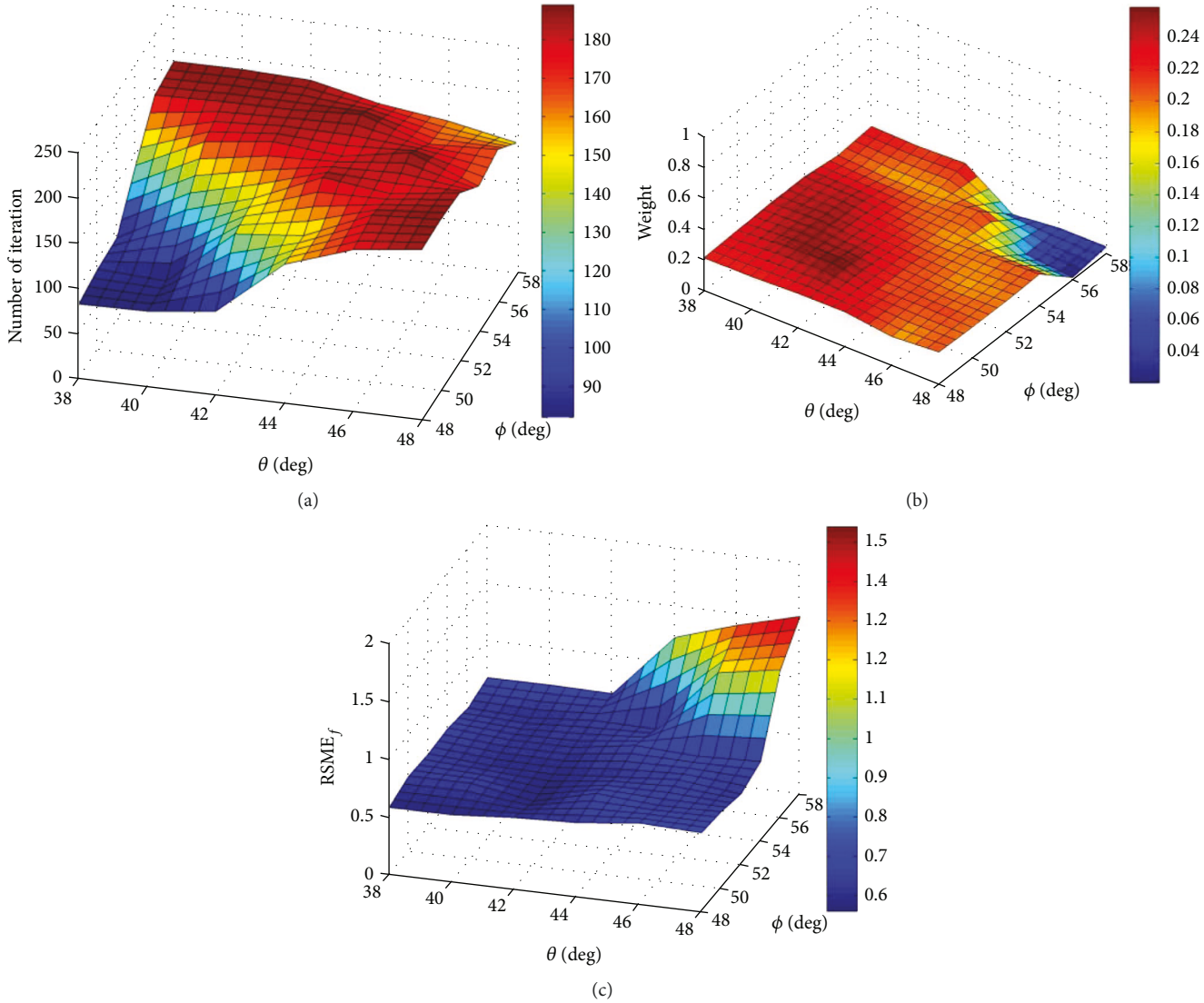

Figure 10: (a) Number of iteration versus initial position for component B; (b) weight versus initial position for component B; (c) RMSE$_f$ versus initial position for component B.

signal distribution function by the proposed algorithm. The result of the proposed method reflects spatial nonsymmetric distribution of the source and is closer to the given distributed source.

In the second example, we examine the changing processes of Gaussian components during the EM iterations. The initial nominal azimuth and nominal elevation of components A, B, C, and D are (43°, 43°), (43°, 53°), (53°, 43°), and (53°, 53°), respectively. The initial angular spreads are set at 1°. The number of snapshots is set at 200 and SNR is 15 dB. The changing processes of parameters in each component are shown in Figure 6. All parameters converge to certain values after sufficient iterations. As shown in Figure 6(d), a small weight 0.040 is developed by component D, which indicated that the nominal angles of the Gaussian component outside the scope of the distributed source make only a small contribution to the final result.

In the third example, we examine the relationship between the number of Gaussian components and estimation performance. The number of snapshots is set at 200 and SNR is 15 dB. Figure 7 shows that the error is large when there is only one Gaussian component. It can be found that RMSE$_f$ and RMSE$_a$ decrease as Gaussian components increase. Both the final RMSE$_f$ and final RMSE$_a$ change slightly as the number of Gaussian components changes from 3 to 6, and the convergence is markedly slow, which shows that increasing the number of Gaussian components will improve accuracy of estimation. Nevertheless, the effect will not be significantly improved as the number exceeds a certain extent.

The initial position parameters may be set around the guessed values; there will be initial Gaussian components outside the distributed source inevitably. To increase the robustness of the algorithm, the number of Gaussian

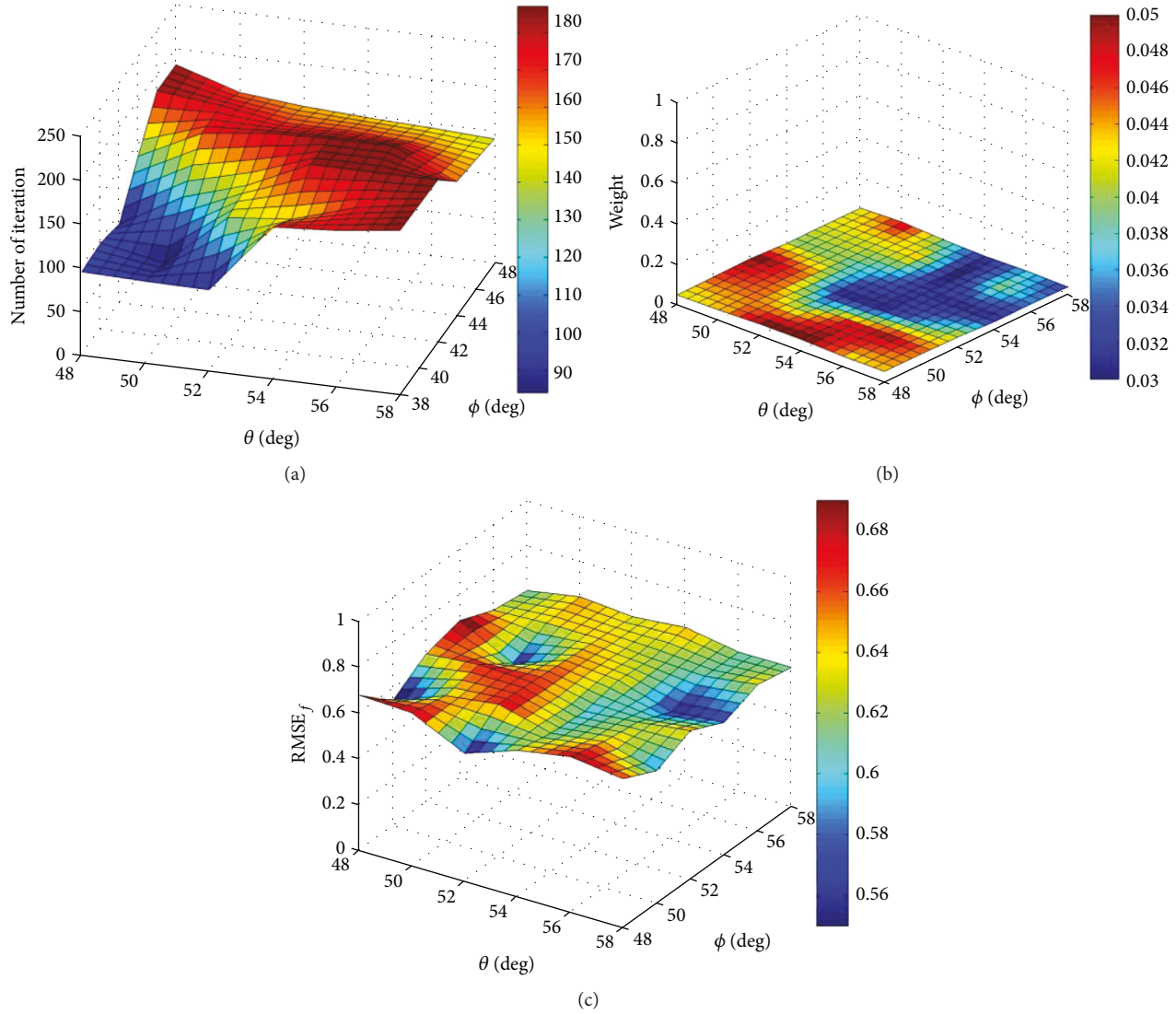

FIGURE 11: (a) Number of iteration versus initial position for component C; (b) weight versus initial position for component C; (c) RMSE$_f$ versus initial position for component C.

components should be selected from a larger range; meanwhile, computing cost is a matter of balance.

In the fourth example, we examine the relationship between the initial positions of Gaussian components and estimation results. The initial positions of component A, B, C, and D are considered taking values within squares where the centers are set at (43°, 43°), (43°, 53°), (53°, 43°), and (53°, 53°). Initial weights are all set at 0.25. Each square takes 400 values uniformly. Figure 8 shows the investigated region of initial positions, where the purple region is the projection of the constructed nonsymmetric angular signal distribution function (45) on the θ-ϕ plane, and the color bar represents measurement of PDF. We investigate the influence of the initial position of a component on the number of iterations, final weight of the component, and RMSE$_f$ while initial positions of other components are set at centers. It should be noted that weights and positions of components would be changing during EM iterations, which have been shown in the second example. We focus on the sensitivity of initial positions to the final results; the weight and RMSE$_f$ can be persuasive. The stopping criterion of the EM algorithm is the iterative variation $\delta \leq 0.01$.

Figure 9(a) shows that initial positions of component A in the lower left part of the square have fewer iterations. The initial positions closer to the distributed source tend to have faster convergence rates. As shown in Figure 9(b), weights change slightly in the whole region. It can be concluded that the contribution of component A to the final PDF is stable when the initial positions are set in the investigated range. Figure 9(c) shows RMSE$_f$s change at a low level and in a small range, which means estimations maintain good accuracy with initial positions in the square.

Figure 10(a) shows that initial positions of component B in the lower left part and upper right part have fewer

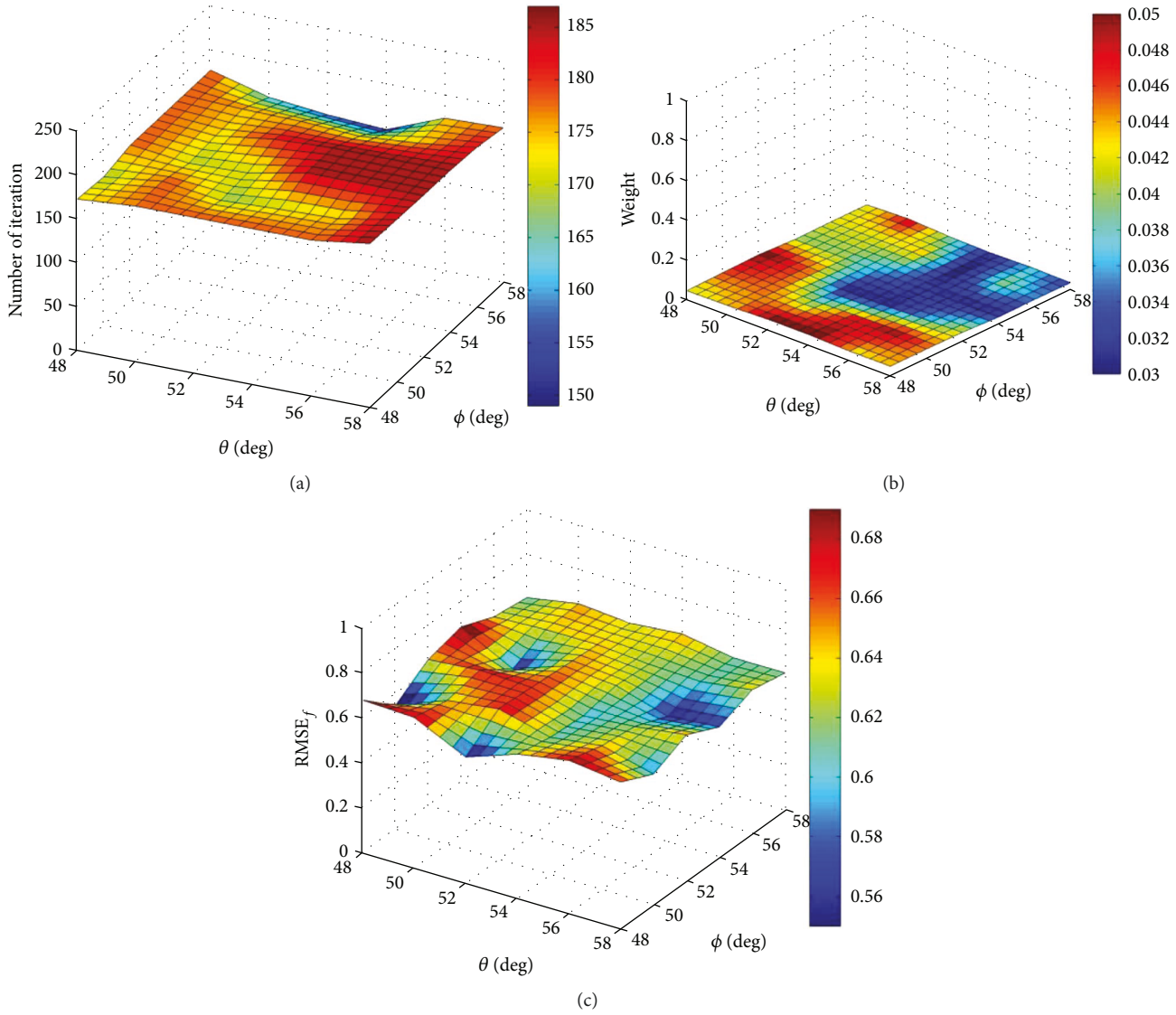

FIGURE 12: (a) Number of iteration versus initial position for component D; (b) weight versus initial position for component D; (c) RMSE_f versus initial position for component D.

iterations. The lower left part has faster convergence rate due to closer distances from initial positons to the distributed source. The upper right part shows that the convergence rates increase when the distances from the initial positions to the distributed source exceed a certain degree. The weights in the upper right part decrease significantly in Figure 10(b), which implies that component B with initial positions in this part has little contribution to estimation result; consequently, RMSE_fs increase remarkably in Figure 10(c).

From Figure 11, we can find that the influence of initial positions of component C on the estimation results is similar to that of component B in respective regions. The lower left part which is close to the distributed source and the upper right part which is far from the distributed source have fewer iterations. As the similar region of component B, the upper right part of component C has small weights and large RMSE_fs.

Figure 12 shows that numbers of iterations, weights of component D, and the distribution errors vary indistinctively in the whole range. No matter where the initial position is taken for component D, it is far away from the distributed source. From the example of components A, B, C, and D, it can be drawn that although the initial positions closer to distributed source have faster convergence rates, the weights and RMSE_fs tend to be stable until the distances from the initial positions to the distributed source exceed a certain degree. When the distances exceed a robust range, the convergence rates increase, the weights decrease, and RMSE_fs increase remarkably. The estimation of a 2D nonsymmetric CD source by the proposed algorithm shows robustness with regard to initial position of the Gaussian component.

5. Conclusions

In this study, we have considered the problem of estimating a nonsymmetric 2D CD source under L-shaped arrays. The

method we proposed is developed by modeling the nonsymmetric deterministic angular signal distribution function as Gaussian mixture. Parameters of a nonsymmetric CD source are more than those of a symmetric CD source. Parameter estimation based on an iterative EM framework has been introduced in detail. The computational cost of estimation for a nonsymmetric CD source is much higher compared with that of a symmetric CD source. For the sake of evaluating the estimation, two indicators are defined, and one reflects nominal angles and another for spatial distribution. Simulation results indicated that the proposed method is effective and robust for the estimation of a nonsymmetric CD source.

Appendix

A. Appendix A

Change the variables $(\theta_i + \tilde{\theta})$ for θ and $(\phi_i + \tilde{\phi})$ for ϕ, where $\tilde{\theta}$ and $\tilde{\phi}$ are the small deviations of θ_i and ϕ_i. Thus, $\cos\theta \sin\phi$ and $\sin\theta \sin\phi$ can be approximated by the first term in the Taylor series expansions

$$\begin{aligned}
[\boldsymbol{\alpha}_{Ai}(\mathbf{u}_i)]_k &= \iint g_i(\theta,\phi;\mathbf{u}_i) e^{j2\pi d(k-1)\cos\theta\sin\phi/\lambda} d\tilde{\theta}d\tilde{\phi} \\
&\approx \iint g_i(\theta,\phi;\mathbf{u}_i) e^{j\pi(k-1)\left(\cos\theta_i\sin\phi_i+\cos\theta_i\cos\phi_i\tilde{\phi}-\sin\theta_i\sin\phi_i\tilde{\theta}\right)} d\tilde{\theta}d\tilde{\phi} \\
&= e^{j\pi(k-1)\cos\theta_i\sin\phi_i} \iint g_i(\theta,\phi;\mathbf{u}_i) e^{j\pi(k-1)\left(\cos\theta_i\cos\phi_i\tilde{\phi}-\sin\theta_i\sin\phi_i\tilde{\theta}\right)} d\tilde{\theta}d\tilde{\phi}, \\
[\boldsymbol{\alpha}_{Bi}(\mathbf{u}_i)]_k &= \iint g_i(\theta,\phi;\mathbf{u}_i) e^{j2\pi d(k-2)\cos\theta\sin\phi/\lambda} d\tilde{\theta}d\tilde{\phi} \\
&\approx \iint g_i(\theta,\phi;\mathbf{u}_i) e^{j\pi(k-2)\left(\cos\theta_i\sin\phi_i+\cos\theta_i\cos\phi_i\tilde{\phi}-\sin\theta_i\sin\phi_i\tilde{\theta}\right)} d\tilde{\theta}d\tilde{\phi} \\
&= e^{j\pi(k-2)\cos\theta_i\sin\phi_i} \iint g_i(\theta,\phi;\mathbf{u}_i) e^{-j\pi\left(\cos\theta_i\cos\phi_i\tilde{\phi}-\sin\theta_i\sin\phi_i\tilde{\theta}\right)} e^{j\pi(k-1)\left(\cos\theta_i\cos\phi_i\tilde{\phi}-\sin\theta_i\sin\phi_i\tilde{\theta}\right)} d\tilde{\theta}d\tilde{\phi}.
\end{aligned} \tag{47}$$

Considering $\tilde{\theta}$ and $\tilde{\phi}$ are small variables, so we have

$$e^{-j\pi\left(\cos\theta_i\cos\phi_i\tilde{\phi}-\sin\theta_i\sin\phi_i\tilde{\theta}\right)} \approx 1. \tag{48}$$

Thus, we can obtain following relationship

$$\boldsymbol{\alpha}_{Ai}(\mathbf{u}_i) \approx e^{j\pi\cos\theta_i\sin\phi_i}\boldsymbol{\alpha}_{Bi}(\mathbf{u}_i). \tag{49}$$

Similarly,

$$\begin{aligned}
[\boldsymbol{\beta}_{Ai}(\mathbf{u}_i)]_k &= \iint g_i(\theta,\phi;\mathbf{u}_i) e^{j2\pi d(k-1)\sin\theta\sin\phi/\lambda} d\tilde{\theta}d\tilde{\phi} \\
&\approx \iint g_i(\theta,\phi;\mathbf{u}_i) e^{j\pi(k-1)\left(\sin\theta_i\sin\phi_i+\sin\theta_i\cos\phi_i\tilde{\phi}+\cos\theta_i\sin\phi_i\tilde{\theta}\right)} d\tilde{\theta}d\tilde{\phi} \\
&= e^{j\pi(k-1)\sin\theta_i\sin\phi_i} \iint g_i(\theta,\phi;\mathbf{u}_i) e^{j\pi(k-1)\left(\sin\theta_i\cos\phi_i\tilde{\phi}+\cos\theta_i\sin\phi_i\tilde{\theta}\right)} d\tilde{\theta}d\tilde{\phi}, \\
[\boldsymbol{\beta}_{Bi}(\mathbf{u}_i)]_k &= \iint g_i(\theta,\phi;\mathbf{u}_i) e^{j2\pi d(k-2)\sin\theta\sin\phi/\lambda} d\tilde{\theta}d\tilde{\phi} \\
&\approx \iint g_i(\theta,\phi;\mathbf{u}_i) e^{j\pi(k-2)\left(\sin\theta_i\sin\phi_i+\sin\theta_i\cos\phi_i\tilde{\phi}+\cos\theta_i\sin\phi_i\tilde{\theta}\right)} d\tilde{\theta}d\tilde{\phi} \\
&= e^{j\pi(k-2)\sin\theta_i\sin\phi_i} \iint g_i(\theta,\phi;\mathbf{u}_i) e^{-j\pi\left(\sin\theta_i\cos\phi_i\tilde{\phi}+\cos\theta_i\sin\phi_i\tilde{\theta}\right)} e^{j\pi(k-1)\left(\sin\theta_i\cos\phi_i\tilde{\phi}+\cos\theta_i\sin\phi_i\tilde{\theta}\right)} d\tilde{\theta}d\tilde{\phi}.
\end{aligned} \tag{50}$$

Consider the following relationship:

$$e^{-j\pi\left(\sin\theta_i\cos\phi_i\tilde{\phi}+\cos\theta_i\sin\phi_i\tilde{\theta}\right)} \approx 1. \tag{51}$$

So we have

$$\boldsymbol{\beta}_{Ai}(\mathbf{u}_i) \approx e^{j\pi\sin\theta_i\sin\phi_i}\boldsymbol{\beta}_{\mathrm{Bi}}(\mathbf{u}_i). \tag{52}$$

B. Appendix B

$$
\begin{aligned}
[\boldsymbol{\alpha}_i(\mathbf{u}_i)]_k &= \iint \frac{1}{2\pi\sigma_i^2} e^{-0.5\left[\left(\frac{\theta-\theta_i}{\sigma_i}\right)^2+\left(\frac{\phi-\phi_i}{\sigma_i}\right)^2\right]} e^{j\pi(k-1)\cos\theta\sin\phi} d\theta d\phi \\
&\approx \iint \frac{1}{2\pi\sigma_i^2} e^{-0.5\left[\left(\frac{\tilde{\theta}}{\sigma_i}\right)^2+\left(\frac{\tilde{\phi}}{\sigma_i}\right)^2\right]} e^{j\pi(k-1)\left(\cos\theta_i\sin\phi_i+\cos\theta_i\cos\phi_i\tilde{\phi}-\sin\theta_i\sin\phi_i\tilde{\theta}\right)} d\tilde{\theta}d\tilde{\phi} \\
&= e^{j\pi(k-1)\cos\theta_i\sin\phi_i} \iint \frac{1}{2\pi\sigma_i^2} e^{-0.5\left[\left(\frac{\tilde{\theta}}{\sigma_i}\right)^2+\left(\frac{\tilde{\phi}}{\sigma_i}\right)^2-2j\pi(k-1)\left(\cos\theta_i\cos\phi_i\tilde{\phi}-\sin\theta_i\sin\phi_i\tilde{\theta}\right)\right]} d\tilde{\theta}d\tilde{\phi} \\
&= e^{j\pi(k-1)\cos\theta_i\sin\phi_i} e^{-0.5\left\{[\pi\sigma_i(k-1)\sin\theta_i\sin\phi_i]^2+[\pi\sigma_i(k-1)\cos\theta_i\cos\phi_i]^2\right\}}, \\
[\boldsymbol{\beta}_i(\mathbf{u}_i)]_k &= \iint \frac{1}{2\pi\sigma_i^2} e^{-0.5\left[\left(\frac{\theta-\theta_i}{\sigma_i}\right)^2+\left(\frac{\phi-\phi_i}{\sigma_i}\right)^2\right]} e^{j\pi(k-1)\sin\theta\sin\phi} d\theta d\phi \\
&\approx \iint \frac{1}{2\pi\sigma_i^2} e^{-0.5\left[\left(\frac{\tilde{\theta}}{\sigma_i}\right)^2+\left(\frac{\tilde{\phi}}{\sigma_i}\right)^2\right]} e^{j\pi(k-1)\left(\sin\theta_i\sin\phi_i+\sin\theta_i\cos\phi_i\tilde{\phi}+\cos\theta_i\sin\phi_i\tilde{\theta}\right)} d\tilde{\theta}d\tilde{\phi} \\
&= e^{j\pi(k-1)\sin\theta_k\sin\phi_k} \iint \frac{1}{2\pi\sigma_i^2} e^{-0.5\left[\left(\frac{\tilde{\theta}}{\sigma_i}\right)^2+\left(\frac{\tilde{\phi}}{\sigma_i}\right)^2-2j\pi(k-1)\left(\sin\theta_i\cos\phi_i\tilde{\phi}+\cos\theta_i\sin\phi_i\tilde{\theta}\right)\right]} d\tilde{\theta}d\tilde{\phi} \\
&= e^{j\pi(k-1)\sin\theta_k\sin\phi_k} e^{-0.5\left\{[\pi\sigma_i(k-1)\cos\theta_i\sin\phi_i]^2+[\pi\sigma_i(k-1)\sin\theta_i\cos\phi_i]^2\right\}}.
\end{aligned}
\tag{53}
$$

Conflicts of Interest

The authors declare that they have no conflicts of interest.

Acknowledgments

This work was supported by the Chinese National Science Foundation under Grant no. 61471299.

References

[1] S. Valaee, B. Champagne, and P. Kabal, "Parametric localization of distributed sources," *IEEE Transactions on Signal Processing*, vol. 43, no. 9, pp. 2144–2153, 1995.

[2] Y. Meng, P. Stoica, and K. M. Wong, "Estimation of the directions of arrival of spatially dispersed signals in array processing," *IEE Proceedings - Radar, Sonar and Navigation*, vol. 143, no. 1, p. 1, 1996.

[3] Q. Wu, K. M. Wong, Y. Meng, and W. Read, "Doa estimation of point and scattered sources - vet-music," in *IEEE Seventh SP Workshop on Statistical Signal and Array Processing*, pp. 365–368, Quebec, City, QC, Canada, June 1994.

[4] S. Shahbazpanahi, S. Valaee, and M. H. Bastani, "Distributed source localization using ESPRIT algorithm," *IEEE Transactions on Signal Processing*, vol. 49, no. 10, pp. 2169–2178, 2001.

[5] A. Zoubir and Y. Wang, "Efficient DSPE algorithm for estimating the angular parameters of coherently distributed sources," *Signal Processing*, vol. 88, no. 4, pp. 1071–1078, 2008.

[6] A. Zoubir, Y. Wang, and P. Charge, "New adaptive beamformers for estimation of spatially distributed sources," in *IEEE Antennas and Propagation Society Symposium, 2004*, vol. 3, pp. 2643–2646, Monterey, CA, USA, June 2004.

[7] A. Zoubir and Y. Wang, "Performance analysis of the generalized beamforming estimators in the case of coherently distributed sources," *Signal Processing*, vol. 88, no. 2, pp. 428–435, 2008.

[8] X. Wenmeng, P. José, and M. Sylvie, "Performance analysis of distributed source parameter estimator (DSPE) in the presence of modeling errors due to the spatial distributions of sources," *Signal Processing*, vol. 143, pp. 146–151, 2018.

[9] W. Xiong, J. Picheral, and S. Marcos, "Array geometry impact on music in the presence of spatially distributed sources," *Digital Signal Processing*, vol. 63, pp. 155–163, 2017.

[10] Y. Wang and A. Zoubir, "Some new techniques of localization of spatially distributed sources," in *2007 Conference Record of the Forty-First Asilomar Conference on Signals, Systems and Computers*, pp. 1807–1811, Pacific Grove, CA, USA, November 2007.

[11] S. R. Lee, I. Song, T. Chang, and M. S. Lee, "Distributed source location estimation using a circular array," in *Fourth International Symposium on Signal Processing and Its Applications*, vol. 1, pp. 341–344, Gold Coast, Queensland, Australia, August 1996.

[12] S. R. Lee, I. Song, Y. U. Lee, and H. G. Kim, "Estimation of distributed elevation and azimuth angles using linear arrays," in *Military Communications Conference, 1996. MILCOM '96, Conference Proceedings, IEEE*, vol. 3, pp. 868–872, McLean, VA, USA, October 1996.

[13] Q. Wan and Y.-N. Peng, "Low-complexity estimator for four-dimensional parameters under a reparameterised distributed source model," *IEE Proceedings - Radar, Sonar and Navigation*, vol. 148, no. 6, pp. 313–317, 2001.

[14] Q. Wan and W.-l. Yang, "Low-complexity estimator for two-dimensional DOA under a distributed source model," in *2001 CIE International Conference on Radar Proceedings (Cat No.01TH8559)*, pp. 814–818, Beijing, China, October 2001.

[15] K. Han and A. Nehorai, "Nested array processing for distributed sources," *IEEE Signal Processing Letters*, vol. 21, no. 9, pp. 1111–1114, 2014.

[16] G. M. Zhang and H. G. Wang, "A parameter estimation method of 2D distributed source based on L-shape uniform array," *Technical Acoustics*, vol. 33, pp. 204–208, 2014.

[17] Z. Gaoyi and T. Bin, "Decoupled estimation of 2D DOA for coherently distributed sources using 3D matrix pencil method," *EURASIP Journal on Advances in Signal Processing*, vol. 2008, no. 1, Article ID 417157, 2008.

[18] J. Lee, I. Song, H. Kwon, and S. Ro Lee, "Low-complexity estimation of 2D DOA for coherently distributed sources," *Signal Processing*, vol. 83, no. 8, pp. 1789–1802, 2003.

[19] Z. Zheng, G. J. Li, and Y. L. Teng, "Low-complexity method for the 2D DOA decoupled estimation of coherently distributed sources," *Chinese Journal of Radio Science*, vol. 25, pp. 527–533, 2010.

[20] X. S. Guo, Q. Wan, W. L. Yang, and X. M. Lei, "Low-complexity 2D coherently distributed sources decoupled DOAs estimation method," *Science in China Series F: Information Sciences*, vol. 52, no. 5, pp. 835–842, 2009.

[21] Z. Zheng, G. Li, and Y. Teng, "Simplified estimation of 2D DOA for coherently distributed sources," *Wireless Personal Communications*, vol. 62, no. 4, pp. 907–922, 2012.

[22] Z. Zheng, G. Li, and Y. Teng, "2D DOA estimator for multiple coherently distributed sources using modified propagator," *Circuits, Systems, and Signal Processing*, vol. 31, no. 1, pp. 255–270, 2012.

[23] Z. Zheng, G. Li, and Y. Teng, "Low-complexity 2D DOA estimator for multiple coherently distributed sources," *COMPEL - The International Journal for Computation and Mathematics in Electrical and Electronic Engineering*, vol. 31, no. 2, pp. 443–459, 2012.

[24] L. Wan, G. Han, J. Jiang, C. Zhu, and L. Shu, "A DOA estimation approach for transmission performance guarantee in D2D communication," *Mobile Networks and Applications*, vol. 22, no. 6, pp. 998–1009, 2017.

[25] Z. Dai, W. Cui, B. Ba, D. Wang, and Y. Sun, "Two-dimensional DOA estimation for coherently distributed sources with symmetric properties in crossed arrays," *Sensors*, vol. 17, no. 6, article 1300, 2017.

[26] X. Yang, Z. Zheng, C. C. Ko, and L. Zhong, "Low-complexity 2D parameter estimation of coherently distributed noncircular signals using modified propagator," *Multidimensional Systems and Signal Processing*, vol. 28, no. 2, pp. 407–426, 2017.

[27] X. Yang, G. Li, Z. Zheng, and L. Zhong, "2D DOA estimation of coherently distributed noncircular sources," *Wireless Personal Communications*, vol. 78, no. 2, pp. 1095–1102, 2014.

[28] S. Kikuchi, H. Tsuji, and A. Sano, "Direction-of-arrival estimation for spatially non-symmetric distributed sources," in *Processing Workshop Proceedings, 2004 Sensor Array and Multichannel Signal*, pp. 589–593, Barcelona, Spain, July 2004.

[29] H. Wang, S. Li, Y. Shi, and H. Li, "Gaussian mixture model approximation of total spatial power spectral density for multiple incoherently distributed sources," *IET Signal Processing*, vol. 7, no. 4, pp. 306–311, 2013.

[30] T. K. Moon, "The expectation-maximization algorithm," *IEEE Signal Processing Magazine*, vol. 13, no. 6, pp. 47–60, 1996.

[31] M. I. Miller and D. R. Fuhrmann, "Maximum-likelihood narrow-band direction finding and the EM algorithm," *IEEE Transactions on Acoustics, Speech, and Signal Processing*, vol. 38, no. 9, pp. 1560–1577, 1990.

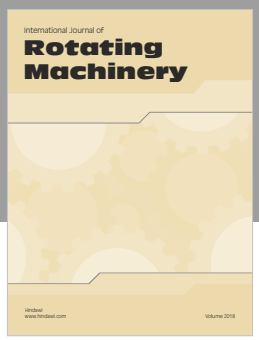

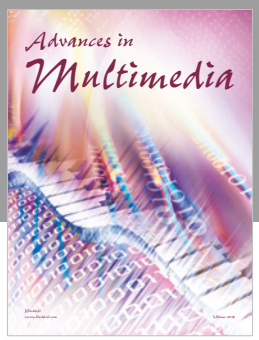

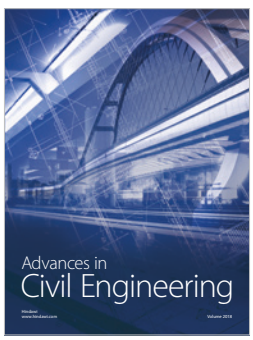

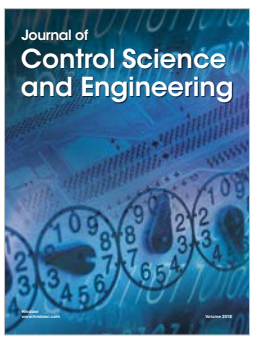

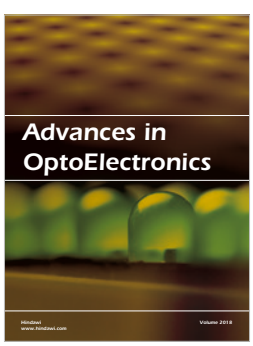

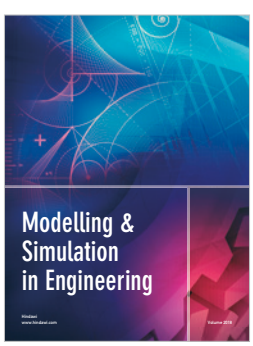

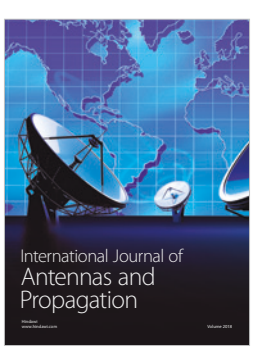

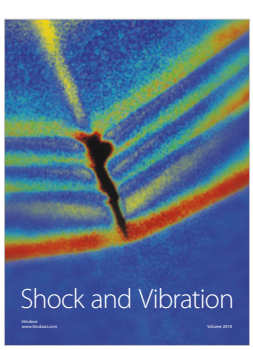

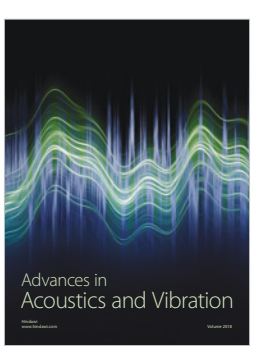

Hindawi

Submit your manuscripts at
www.hindawi.com